Remote Sensing of Environment 300 (2024) 113917

Contents lists available at ScienceDirect

Remote Sensing of Environment

journal homepage: www.elsevier.com/locate/rse

Evaluating the spatial patterns of U.S. urban NOx emissions using TROPOMI NO_2

Daniel L. Goldberg [a,*], Madankui Tao [b], Gaige Hunter Kerr [a], Siqi Ma [c], Daniel Q. Tong [c], Arlene M. Fiore [d], Angela F. Dickens [e], Zachariah E. Adelman [e], Susan C. Anenberg [a]

[a] Department of Environmental and Occupational Health, Milken Institute of Public Health, George Washington University, Washington, DC, USA
[b] Department of Earth and Environmental Sciences, Columbia University, New York City, NY, USA
[c] Department of Atmospheric, Oceanic & Earth Sciences, George Mason University, Fairfax, VA, USA
[d] Department of Earth, Atmospheric, and Planetary Sciences, Massachusetts Institute of Technology, Cambridge, MA, USA
[e] Lake Michigan Air Directors Consortium, Hillside, IL, USA

A B S T R A C T

Satellite nitrogen dioxide (NO_2) datasets are increasingly used to evaluate nitrogen oxides (NOx) emissions inventories. Such studies often use a chemical transport model or a complex statistical framework involving an assumed NO_2 lifetime, which can complicate the comparison. Here, we apply a novel method to compare inventory-based NOx emissions directly to Tropospheric Monitoring Instrument (TROPOMI) NO_2 data without a chemical transport model by only using measurements during stagnant wind days. We oversample the satellite data over multiple years filtering to include data when near-surface wind speeds are <3.2 m/s, and then use this filtered dataset to evaluate the spatial representativeness of the 1×1 km^2 inventory-based Neighborhood Emission Mapping Operation (NEMO). In nine out of ten US cities evaluated, spatial r^2-values between NEMO NOx emissions and TROPOMI NO_2 exceeded 0.73. This suggests that the 108 spatial surrogates used by NEMO to spatially disaggregate NOx emissions from the U.S. county-level (5–200 km length scale) to the neighborhood level (~1 km length scale) are generally appropriate. However, areas with dense intermodal facilities, such as railyards and warehouses, appear to underestimate NOx emissions. Additionally, we find some evidence that NOx emissions in wealthy communities appear to be overestimated by the standard surrogates used to disaggregate the inventory. This work provides a basis for the direct use of satellite data for evaluating the spatial patterns of urban NOx emissions inventories.

1. Introduction

Nitrogen dioxide (NO_2) is an air pollutant that adversely affects the human respiratory system (Health Effects Institute, 2022; Khreis et al., 2017) and leads to premature mortality (Burnett et al., 2004; He et al., 2020). NO_2 is also an important precursor for ozone and fine particulates, which also have serious health impacts. In urban areas, the majority of ambient NO_2 originates from NOx emissions (=NO+NO_2; most NOx is emitted as NO which rapidly cycles to NO_2) during high-temperature fossil fuel combustion (Crippa et al., 2021). In many circumstances, end-of-pipe controls such as automotive catalytic converters (Koltsakis and Stamatelos, 1997) and selective catalytic reduction (Busca et al., 1998) can reduce the amount of NOx emitted from engines and boilers by 70–99% but these technologies do not recover 100% of the NOx generation during combustion. Because of this, NO_2 accumulates in cities and most urban areas have NO_2 concentrations that exceed the World Health Organization guideline of 5.3 ppb for an annual average (Anenberg et al., 2022).

To cost-effectively control NO_2, it is important to precisely know where NO_2 originates in cities. Mapping NOx emissions typically requires selecting emissions rates or factors for each source and distributing the sources using spatial surrogates; both steps introduce considerable uncertainty into the estimates. While the types of activities that emit NOx are known well (e.g., vehicles, fossil-fuel-fired power plants, etc.), not all vehicles or power plants have identical NOx emissions and the magnitude of NOx emissions from any source can vary dramatically by geographic region (Crippa et al., 2018; Janssens-Maenhout et al., 2015; McDuffie et al., 2020). Typically, NOx emissions for an area are estimated by summing up the amount of fuel burned in that area and using sector-specific emissions factors or rates (McDuffie et al., 2020); for example, there are different emissions for vehicles versus industrial boilers, given the same mass of fuel burned. In some countries, such as India (Guttikunda et al., 2019; Saw et al., 2021), accurate data on fossil fuel consumption and sector emission rates are difficult to acquire. In other countries, fossil fuel consumption and sector emission rates can be accurate for national (~1000 km) or regional (~100 km) spatial scales, but additional information is needed to estimate NOx emissions rates at neighborhood (~1 km) scales. Spatial

* Corresponding author.
E-mail address: dgoldberg@gwu.edu (D.L. Goldberg).

https://doi.org/10.1016/j.rse.2023.113917
Received 16 March 2023; Received in revised form 7 November 2023; Accepted 10 November 2023
Available online 18 November 2023

surrogates are used to distribute county-level totals into sub-county levels, such as 12 km or 4 km grids (Eyth et al., 2006). For example, one spatial surrogate is the location of a highway; NOx emissions for roadways are typically allocated based on average miles traveled by a vehicle and the total number and type of vehicles on that type of road. For a regional or sub-regional scale, this assumption is often satisfactory, but much more detailed information is needed when trying to downscale a county-level inventory to individual roadways. Therefore, some of the assumptions used to spatially allocate NOx emissions on a relatively coarse grid (~12 km) break down when trying to estimate NOx emissions at the neighborhood spatial scale (~1 km). An independent way to map NOx emissions – to discern when the original assumptions used to develop urban area NOx emissions are valid – would be helpful to better understand the uncertainty in the originally calculated NOx emissions. Remote sensing of air pollutants in urban areas can sometimes fill this role (Beirle et al., 2011, 2019; Finch et al., 2022; Goldberg et al., 2019a; Goldberg et al., 2019b; F. Liu et al., 2017; Montgomery et al., 2023; Pope et al., 2022; Xue et al., 2022).

NO_2 can be observed by remote sensing instruments due to its unique spectroscopic features within the 405–465 nm wavelength region (Vandaele et al., 1998). The Tropospheric Monitoring Instrument (TROPOMI) (Veefkind et al., 2012), launched in October 2017 aboard the Sentinel 5 Precursor satellite, has been measuring column amounts of NO_2 pollution at 5.5×3.5 km^2 spatial resolution (van Geffen, 2016). Because of this higher spatial resolution over predecessor instruments, such as GOME-2 (40×40 km^2 at nadir) (Richter et al., 2011), and OMI (24×13 km^2 at nadir) (Levelt et al., 2018), TROPOMI has ~50 daily satellite pixel measurements within a typical city (~1000 km^2) during clear skies; prior instruments only have 1–3 daily measurements within the borders of each city. This increased measurement capacity within a city allows us to discern spatial variability undetectable by previous instruments. Further, the data from the satellite instruments can be downscaled using a process called oversampling (de Foy et al., 2009; Sun et al., 2018), which re-grids the irregular satellite pixels to a standard and higher spatial resolution. The spatial resolution is thus effectively increased at the expense of the temporal resolution.

The goal of this project is to understand whether oversampled satellite data can directly inform estimated spatial heterogeneities of NOx emissions on a neighborhood scale, without relying on a chemical transport model (Canty et al., 2015; East et al., 2022; Li et al., 2021) or complex statistical inversion technique that involves assuming an uncertain NO_2 lifetime to derive NO_X emissions (Beirle et al., 2011, 2019, 2023; Chen et al., 2023; Goldberg et al., 2019b; F. Liu et al., 2022; Verstraeten et al., 2018). We oversample the satellite data over multiple years and filter to use data on stagnant wind days only – when the vertical overhead column should best capture the local emission influence – and then use this satellite average to evaluate the spatial representativeness of the 1×1 km^2 inventory-based Neighborhood Emission Mapping Operation (NEMO). This work is driven by recent advancements of both satellite instruments (oversampled pixels at $0.01^\circ \times 0.01^\circ$ resolution with improved signal-to-noise) and inventories (1-km spatial resolution inventories across the U.S). As a bridge, we compare NEMO for selected cities to the Emissions Database for Global Atmospheric Research (EDGAR) inventory often used for global analyses, and NEMO to the satellite annual average with varying wind filters, in order to determine the additional utility of both having a high spatial resolution inventory and filtering the satellite data based on wind speed. The ability to directly compare satellite data to inventories without the need for complex modeling would enable air quality planners to evaluate and improve the NOx inventories they use to support air pollution policy decisions.

2. Methods

2.1. TROPOMI

TROPOMI was launched by the European Space Agency (ESA) for the European Union's Copernicus S5P satellite mission on October 13, 2017. Data from the instrument became available on April 30, 2018, after an approximately 6-month calibration period. The satellite follows a sun-synchronous, low-earth (825 km) orbit with an equator overpass time of approximately 13:30 local solar time. TROPOMI measures total column amounts of several trace gases in the Ultraviolet-Visible-Near Infrared (UV-VIS-NIR) (e.g., NO_2 and HCHO) and Shortwave Infrared (SWIR) (e.g., CO) spectral regions (Veefkind et al., 2012). At nadir, pixel sizes are 3.5×7 km^2 (modified to 3.5×5.5 km^2 on August 6, 2019) with the edges having slightly larger pixels sizes (~14 km wide) across a 2600 km swath, equating to 450 rows (van Geffen et al., 2020). The instrument observes the swath approximately once every second and orbits the Earth in about 100 min, resulting in daily global coverage.

NO_2 slant column densities are derived from radiance measurements in the 405–465 nm spectral window of the UV-VIS-NIR spectrometer (van Geffen et al., 2021). Satellite instruments observe NO_2 by comparing observed spectra with a reference spectrum to derive the amount of NO_2 in the atmosphere between the instrument and the surface; this technique is called differential optical absorption spectroscopy (DOAS) (Platt, 1994). Tropospheric vertical column density data, which represent the vertically integrated number of NO_2 molecules per unit area between the surface and the tropopause, are then calculated by subtracting the stratospheric portion and then converting the tropospheric slant column to a vertical column using an air mass factor (AMF) (Boersma et al., 2011). The AMF is a unitless quantity used to convert the slant column into a vertical column and is a function of the satellite viewing angles, solar angles, the effective cloud radiance fraction and pressure, the vertical profile shape of NO_2 provided by a chemical transport model simulation, and the surface reflectivity (Lorente et al., 2017; Palmer et al., 2001). The operational AMF calculation does not explicitly account for aerosol absorption effects, which are accounted for in the effective cloud radiance fraction (Eskes et al., 2023).

For our analysis we use the TROPOMI NO_2 v2.4 algorithm: reprocessed (May 1, 2018 – July 25, 2022) and offline (July 26, 2022 – April 30, 2023). Updates from v1.3 to v2.3.1 involved modifications to the cloud retrieval scheme (decrease in cloud pressure), surface albedo (to avoid negative cloud fractions), and quality flags (better screening of snow). The net result of the change in tropospheric vertical column NO_2 from v1.3 to v2.3.1 has been reported to be a + 13% increase for cloud-free scenes that varies spatially and is higher in polluted areas (van Geffen et al., 2021). The update from v2.3.1 to v2.4 makes use of a $0.125^\circ \times 0.125^\circ$ Directional Lambertian Equivalent Reflectivity (DLER) climatology derived from TROPOMI observations which replaces an old $0.5^\circ \times 0.5^\circ$ Lambertian Equivalent Reflectivity (LER) dataset used in v2.3.1 (Eskes et al., 2023). The TROPOMI NO_2 v.2.4 product has a documented median low bias of −34.8% in moderately polluted locations ($3–14 \times 10^{15}$ molec/cm^2) when compared to a MAX-DOAS network (Lambert et al., 2023). Prior work has demonstrated a strong correlation between TROPOMI NO_2 column measurements and NO_2 surface concentrations in urban areas (Demetillo et al., 2020; Dressel et al., 2022; Goldberg et al., 2021a).

For the domain-wide comparisons, we screened TROPOMI pixels for quality assurance flag values >0.75 for the period between May 2018 – April 2023, and excluding a "COVID" period which we defined as March 10, 2020 until March 9, 2021. This allowed for 4 full years of oversampled NO_2 data using a consistent algorithm. Single pixel TROPOMI NO_2 uncertainties are assumed to be between 30 and 60% (Liu et al., 2021). Oversampled NO_2 measurements over long timeframes (100s of measurements) are assumed to have a much smaller amount of uncertainty. Boersma et al. (2018) suggest that oversampled values have 39% of a single-pixel uncertainty due to potential errors in the surface albedo,

clouds, a priori NO_2 profile, and aerosols, resulting in an uncertainty range of 12–23%. The value 39% calculated by Boersma et al. (2018) was for OMI, and it is reasonable to think this value would be lower for TROPOMI given recent instrument and algorithm advancements.

For comparison with the annual NOx emissions inventory, we gridded TROPOMI data to a 0.01° × 0.01° resolution, to create a custom "Level-3" data product (Goldberg et al., 2021a). This "Level 3" satellite product was then averaged to the zip code level (1–50 km spatial scales depending on region) for comparison with the NOx emissions inventory.

2.2. ERA5 re-analysis

We use the ERA5 re-analysis (Hersbach et al., 2020) of 100-m wind speed and direction between 16 and 21 UTC, which approximates the overpass time of TROPOMI over the continental United States. The 100-m vertical level is a standard output of the ERA-5 re-analysis. The 100-m wind speeds have a strong linear correlation with other options to filter wind speeds, such as 10-m and 0–500 m average (Sun et al., 2021). After averaging the wind estimates from these six hours together, we match the TROPOMI NO_2 satellite data to the ERA5 wind data, and filter to only use satellite data when the 100-m wind speed is <3.2 m-s^{-1}. The ERA5 re-analysis data products are reported at a 0.25° × 0.25° spatial resolution and the wind speed is interpolated, using bilinear interpolation, to the 0.01° × 0.01° oversampled TROPOMI NO_2 grid.

2.3. NEMO U.S. inventory-based NOx emissions

The Neighborhood Emission Mapping Operation (NEMO)is a 1-km anthropogenic emission dataset in the United States (Ma and Tong, 2022). This inventory uses the spatial surrogates recommended by the U.S. EPA (Eyth et al., 2006) – 108 spatial surrogates in total – to downscale the emissions from the county-level to a 1-km grid. Emissions are the 2017 annual total from the U.S. EPA National Emissions Inventory (NEI). The 2020 NEI incorporates emission changes due to the COVID lockdowns and is not representative of the 2018–2023 timeframe used in this analysis. Any projection of NOx emissions from 2017 to a future year, would rely on some type of assumption and would add additional uncertainty, and is therefore also not appropriate for this analysis. For comparison with the gridded satellite data, the NEMO inventory-based NOx emissions was averaged to the zip code level (~1–100 km^2 spatial scales depending on region) so that both are at the same spatial scale. Within urban areas, NEMO's high-resolution aspect is largely preserved since many zip codes are <10 km^2.

2.4. EDGAR NOx inventory-based emissions

For comparison to NEMO, we use EDGAR version 6.1 inventory for NOx (Joint Research Centre, 2022). This global inventory provides annual NOx emissions at 0.1° × 0.1° spatial resolution from all anthropogenic activities, excluding large scale biomass burning. For the energy related sectors, the activity data are primarily based on statistics from the International Energy Agency. Globally, anthropogenic NOx emissions have been relatively constant since 2012 (McDuffie et al., 2020) and in urban areas, they are dropping at a slow rate of 0–4% per year (Goldberg et al., 2021b). For more information on how the EDGAR inventory is compiled, see (Crippa et al., 2018) with updates for version 6.1 noted here: https://edgar.jrc.ec.europa.eu/index.php/dataset_ap61. Fig. 1 compares the EDGAR inventory to the NEMO inventory in the New York City metropolitan area. The EDGAR inventory at 0.1° × 0.1° is similar to the spatial resolution of a regional chemical transport model simulation at 12 × 12 km^2, and the inventory at 0.5° × 0.5° is similar to the spatial resolution of a global chemical transport model simulation.

2.5. Urban area boundaries

For our ten U.S. focus cities, we define cities using metropolitan statistical areas (MSAs) established by the Office of Management and Budget and used by the U.S. Census Bureau (https://www.whitehouse.gov/wp-content/uploads/2020/03/Bulletin-20-01.pdf). The ten focus cities were selected based on a combination of MSA population size (all are within the top 20 in the U·S) and geographic diversity (e.g., Denver selected over Philadelphia). All zip codes that are located within counties belonging to a particular MSA are used in our analysis. MSAs encompass not only the densely populated urban centers but also outlying suburban areas. For example, the Washington DC MSA includes not only the District of Columbia but also counties in Virginia, Maryland, and West Virginia. When comparing TROPOMI NO_2 to NEMO NOx emissions for the U.S. portion of our study, we transform these datasets from their native ~1 km^2 resolution to zip code averages by averaging all grid cell centroids contained within a given zip code. If zip codes are too small to contain coincident grid cells, we inverse distance weight using the surrounding grid cells following Kerr et al. (2021).

3. Results

3.1. Comparison between TROPOMI NO_2 and the gridded emissions inventories

To compare TROPOMI and NEMO, three additional processing steps are needed to allow a direct comparison. The first step involves filtering satellite data to only include days with low wind speeds. Observed column NO_2 on days with low wind speeds correlate strongly with urban NO_X emissions (Lorente et al., 2019). We select satellite data only on days with 100-m wind speeds <3.2 m-s^{-1} (and effectively cloud-free using a quality assurance value of 0.75 or greater). Stagnant airmasses are defined as airmasses with 10-m wind speeds <3.2 m/s (https://www.arl.noaa.gov/documents/reports/atlas.pdf). Here we use the 100-m wind speed in lieu of the 10-m wind speed, which likely has a minimal effect for this analysis. During the May 2018 – April 2023 period, 11–51% of the days per urban area (min: 11% in Chicago, max: 51% in Phoenix) (Fig. 2) have satellite measurements collocated in time with slow wind speeds, down from approximately 46–82% of all days (i.e., we do not apply a wind speed filter).

We apply this filter because NO_2 plume outflow from upwind sources

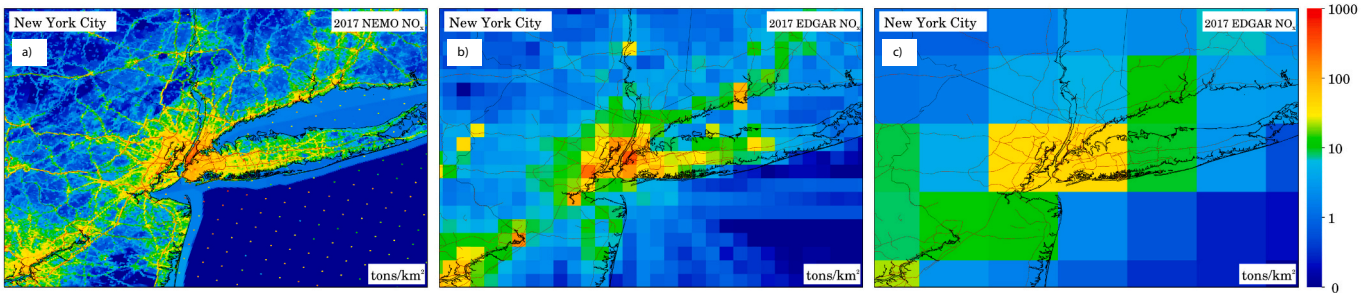

Fig. 1. Annual 2017 NO_X emissions inventories: (a) NEMO (1 × 1 km^2), (b) EDGAR (0.1° × 0.1°), and (c) EDGAR aggregated-up (0.5° × 0.5°).

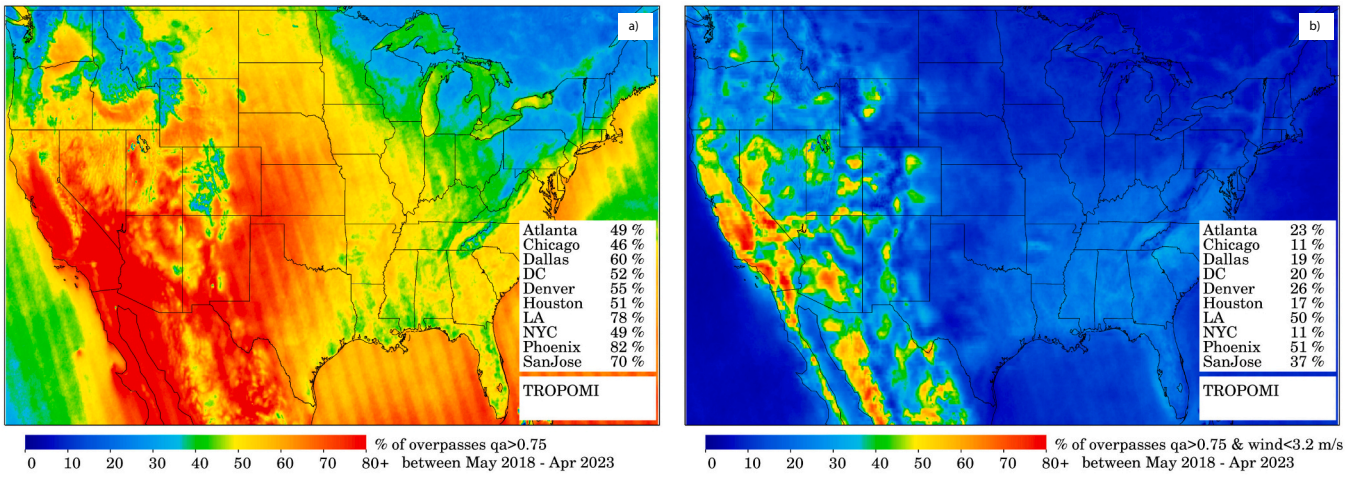

Fig. 2. Percentage of valid TROPOMI measurements using two different filters: (a) filtering for days with the QA value exceeding 0.75 and (b) filtering for days with the qa value exceeding 0.75 and 100-m wind speeds below 3.2 m/s.

on windy days (> 3.2 m/s) can create offsets between surface NOx emissions and observed NO_2 column abundances by the satellite. In Fig. 3, we demonstrate how this filtering affects oversampled NO_2 columns in the Chicago metropolitan area. On days with 100-m wind speeds <3.2 m/s, the NO_2 pollution generally accumulates over land and within the boundaries of Cook County (>5 million residents). On days with 100-m wind speeds >3.2 m/s the NO_2 pollution spreads well out into Lake Michigan, and the NO_2 plume originating from the urban area is more homogenous. The differences in the urban NO_2 spatial heterogeneities between high- and low-wind speed days – while mostly driven by dispersion – could also be partially driven by differences in localized NO_2 lifetimes within the city. For polluted conditions (NO_2 columns > ~ 5 × 10^{15} molec/cm^2), there is a direct relationship between NO_2 lifetime and NO_2 concentrations, (Laughner and Cohen, 2019). Therefore as NO_2 concentrations increase on stagnant wind days a secondary effect of a longer NO_2 lifetime could cause additional accumulation.

In Fig. 3, we also show how a full-year and summer-only (June, July,

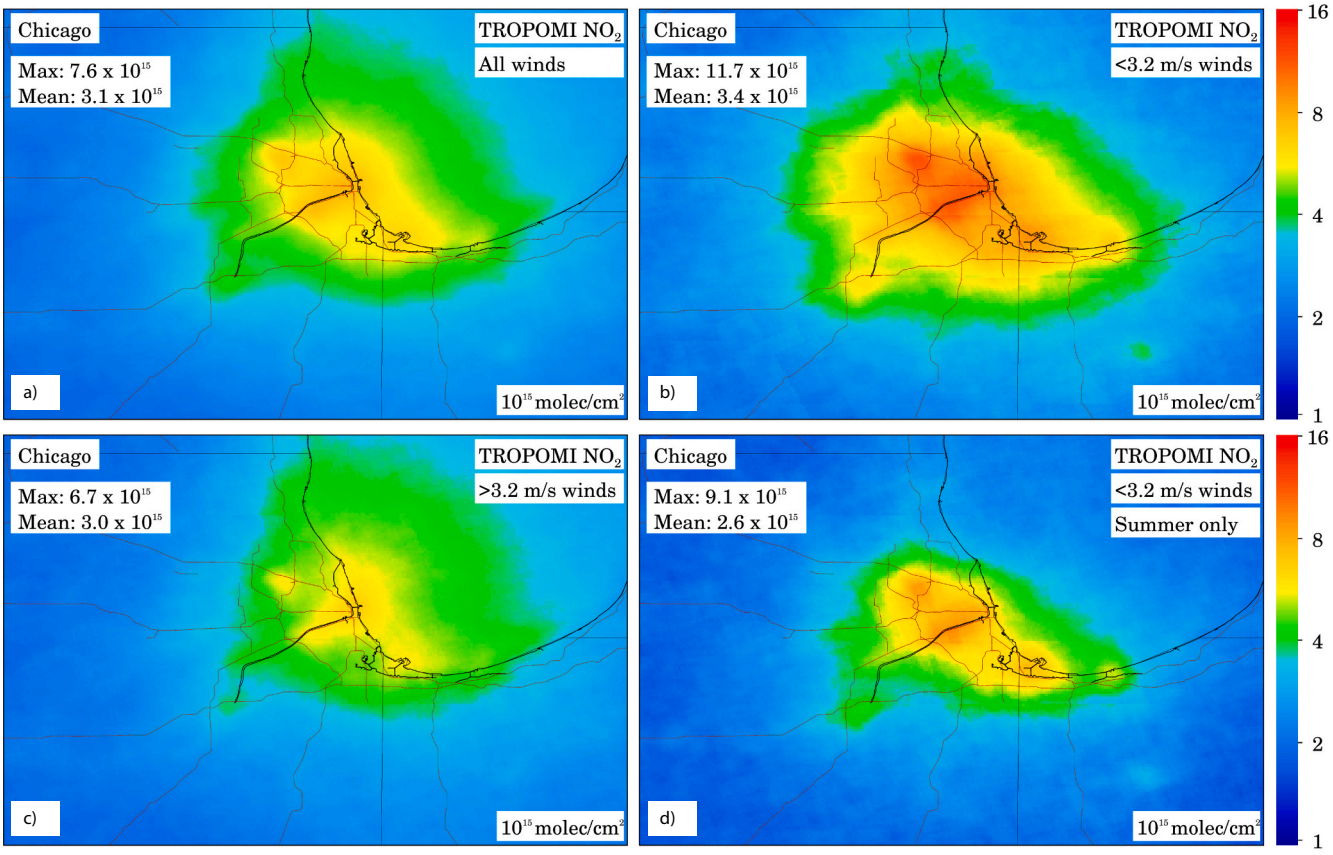

Fig. 3. The oversampled May 2018 – April 2023 average of TROPOMI NO_2 excluding a "COVID" period of March 10, 2020 – March 9, 2021 for various wind and seasonal conditions: (a) all winds and all seasons, (b) stagnant winds <3.2 m/s and all seasons, (c) windy >3.2 m/s and all seasons, and (d) stagnant winds <3.2 m/s and summer (June, July, August).

August) NO_2 oversampled average differ (panel b vs panel d). During summer, the NO_2 lifetime is shorter due to its faster photolytic dissociation. As a result, we see that NO_2 values are smaller during the summer months when compared to a full year average. Also, NO_2 photochemistry within the urban area is relatively similar amongst an average of cloud-free summer-only data compared to a dataset mixing summer and winter measurements. For these reasons, measurements during the summer time could be preferable when intercomparing with the NO_X emissions inventory.

However, there are some downsides to using summer-only data. First, lake/sea/ocean/mountain breezes tend to be stronger on summer days with weak synoptic winds, so filtering for low wind speeds might have a biasing effect that is difficult to control for. Fig. 3 suggests this bias is not large in the Chicago area as the NO_2 plume is not displaced very far inland during the 1:30 PM overpass time; this effect may be larger when using TEMPO data at later hours in the day (Geddes et al., 2021; Wang et al., 2023). Second, limiting to summer-only data reduces the available data in our ten urban areas by about 55–74% as seen in Fig. 4. Using 55–74% fewer measurements in the analysis yields larger uncertainties, since random measurement noise may not be able to be sufficiently averaged out. Third, as denoted in a comparison between the full year and summer-only averages (panel b vs panel d), there is not a drastic difference in the NO_2 spatial gradients when averaging over these two different timeframes. For these reasons, our analysis focuses on year-round data.

Finally, we average both the satellite NO_2 and NOx inventory-based datasets to the zip code level to account for population, for NOx plume conversion to NO_2, and for better TROPOMI sensitivity in urban areas at very fine spatial scales (Goldberg et al., 2022). Although zip codes have varying populations, aggregating to zip code will roughly normalize for population. Zip codes have smaller spatial scales within the center of cities and larger spatial scales in the suburban and peri-urban areas. Since NOx emissions can have significant spatial variation within cities and because the NO_2 background differs from city-to-city, we convert the NO_2 and NOx datasets into units of "percentile rank within the city's metropolitan statistical area" for a more representative intercomparison.

3.2. Urban US Intercomparison: NEMO vs. TROPOMI

We conduct a comparison at the urban scale for ten US cities. In Figs. 5 & 6, we show the inventory-based NOx versus satellite NO_2 intercomparison for all ten cities: Chicago, New York City, Washington DC, Atlanta, Los Angeles (Fig. 5), and Phoenix, Houston, Dallas, Denver, San Francisco (Fig. 6). In the left hand panels, annual inventory-based NOx emissions rates are shown and in the right hand panels the satellite column NO_2 from TROPOMI during stagnant wind (<3.2 m/s at 100-m) days between May 2018 and April 2023, exclusive of a "COVID" March 10, 2020 – March 9, 2021 period are shown. Qualitatively there is spatial agreement between the inventory and satellite column NO_2 measurements for all ten cities; the areas with the largest satellite-observed NO_2 generally correspond to areas with the largest NOx emissions.

We then investigate the differences quantitatively. In Figs. 7 & 8, scatterplots in the left hand column compare the relative zip code percentiles within the MSA between the satellite NO_2 (x-axis) and inventory-based NOx emissions (y-axis) for Chicago, New York City, DC, Atlanta, and Los Angeles. For 9 of the 10 cities (excluding Los Angeles), the r^2-value between the NEMO NOx emissions inventory and TROPOMI NO_2 exceeds 0.73. Despite the strong spatial correlation, there are some neighborhoods within each urban area with disagreements, as shown by the red and blue dots, which correspond to potential inventory overestimates and underestimates respectively. In the middle columns of Figs. 7 & 8, we show the relative difference in percentiles between inventory NOx and satellite NO_2 amongst all zip codes. In the right columns of Figs. 7 & 8, there is the same plot with only the outliers highlighted. Note the different color scales between the middle and right column maps.

For Chicago, we find some notable differences in the inventory-based NOx versus satellite NO_2 intercomparison. First, we observe that some of the point sources in the 2017 inventory are no longer operating in the 2018–2023 timeframe. This led to the largest discrepancies (inventory NOx > satellite NO_2) in two zip codes: 53158 (the location of the former Pleasant Prairie Power Plant, which retired in 2018) and 60087 (the location of the Waukegan Generating Station which has been phasing out and closed in June 2022). Next, we observe discrepancies, potential NOx inventory overestimates, in wealthy neighborhoods on the north side of Chicago. We find a particularly strong NOx overestimate in a zip code within Chicago (60640) that includes Lakeshore Drive highway that prohibits large diesel vehicles. Wealthier residents are more likely to own newer vehicles with better catalytic converters (Federal Highway Administration, 2018; Miller et al., 2002), own newer homes (U.S. Census Bureau, 2022) or have the ability to install home heating energy efficiency measures (Xu and Chen, 2019), own electrified machinery/vehicles (Lee et al., 2019), and have the political capital to minimize emitters, such as diesel trucks, within their neighborhood (Solari, 2012).

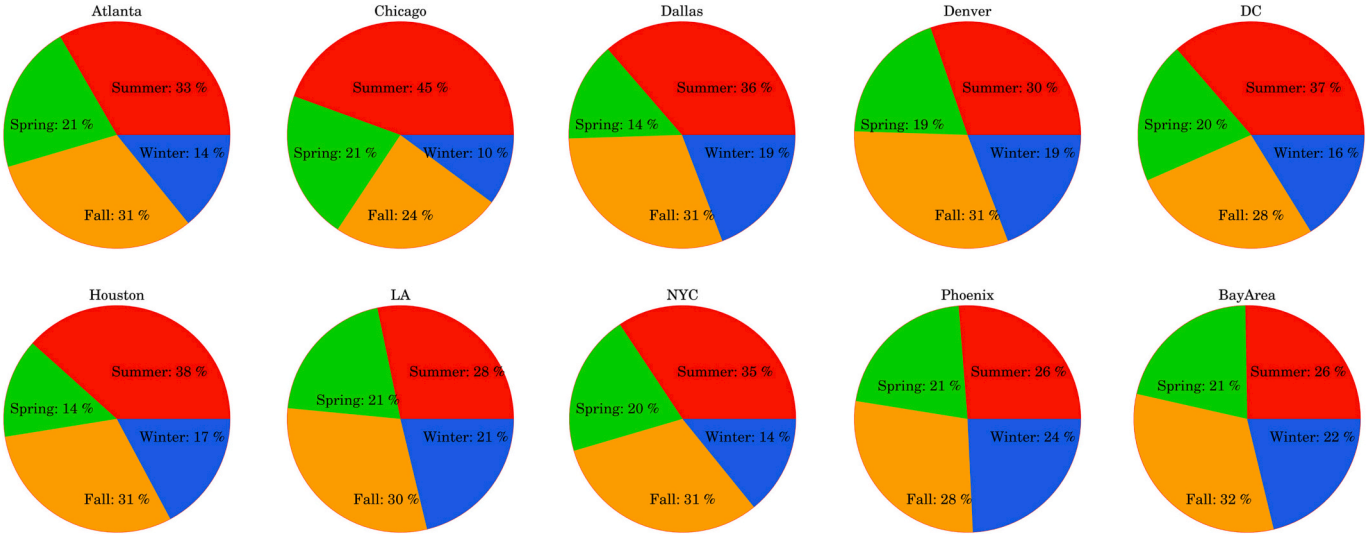

Fig. 4. Seasonal weighting of the "4-year-average" of TROPOMI NO_2 measurements by urban area. Pie charts show the fraction of TROPOMI measurements in each season after filtering using the QA value and low wind speed.

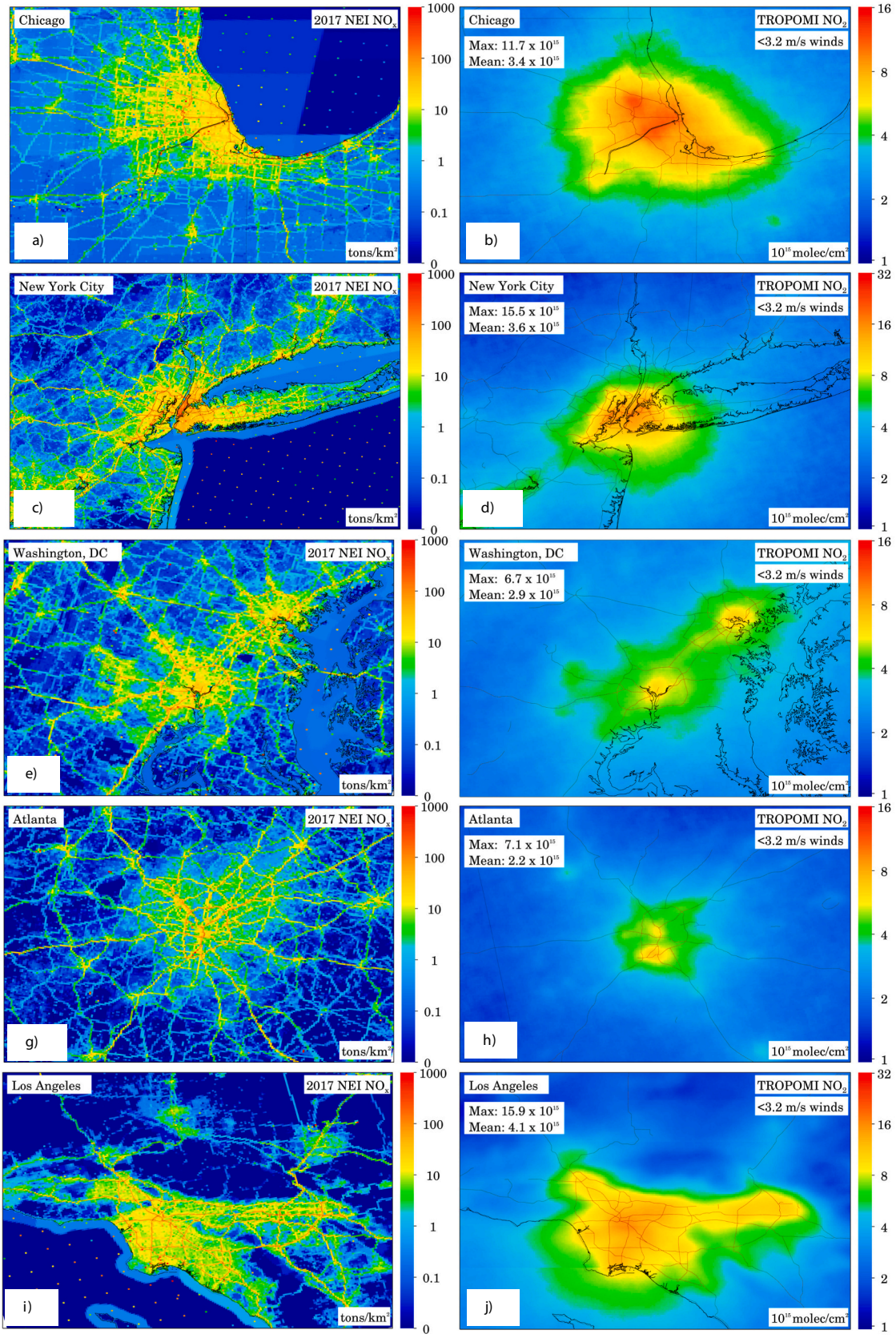

Fig. 5. (Left column) The NEMO NOx emissions inventory for 2017 (Gg/yr NO_2) compared to (Right column) the oversampled May 2018 – April 2023 average of TROPOMI NO_2 during stagnant wind conditions (< 3.2 m/s at 100-m) excluding a "COVID" period of March 10, 2020 – March 9, 2021. The five cities shown are: (Row 1) Chicago, (Row 2) New York City, (Row 3) Washington DC, (Row 4) Atlanta, (Row 5) Los Angeles. Domains are approximately 200–300 km across.

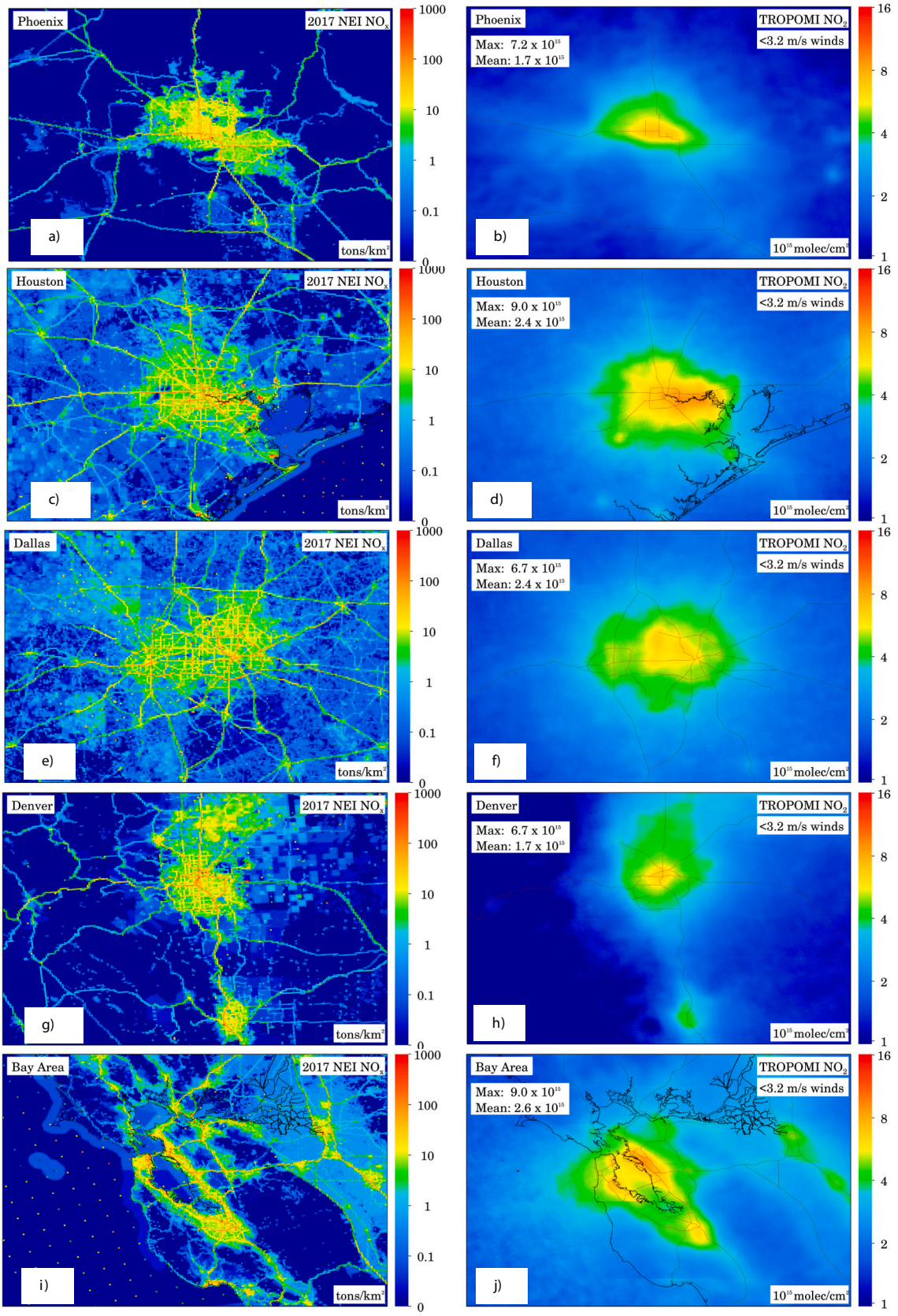

Fig. 6. Same as Fig. 5 but now showing: (Row 1) Phoenix, (Row 2) Houston, (Row 3) Dallas, (Row 4) Denver, and (Row 5) San Francisco Bay Area.

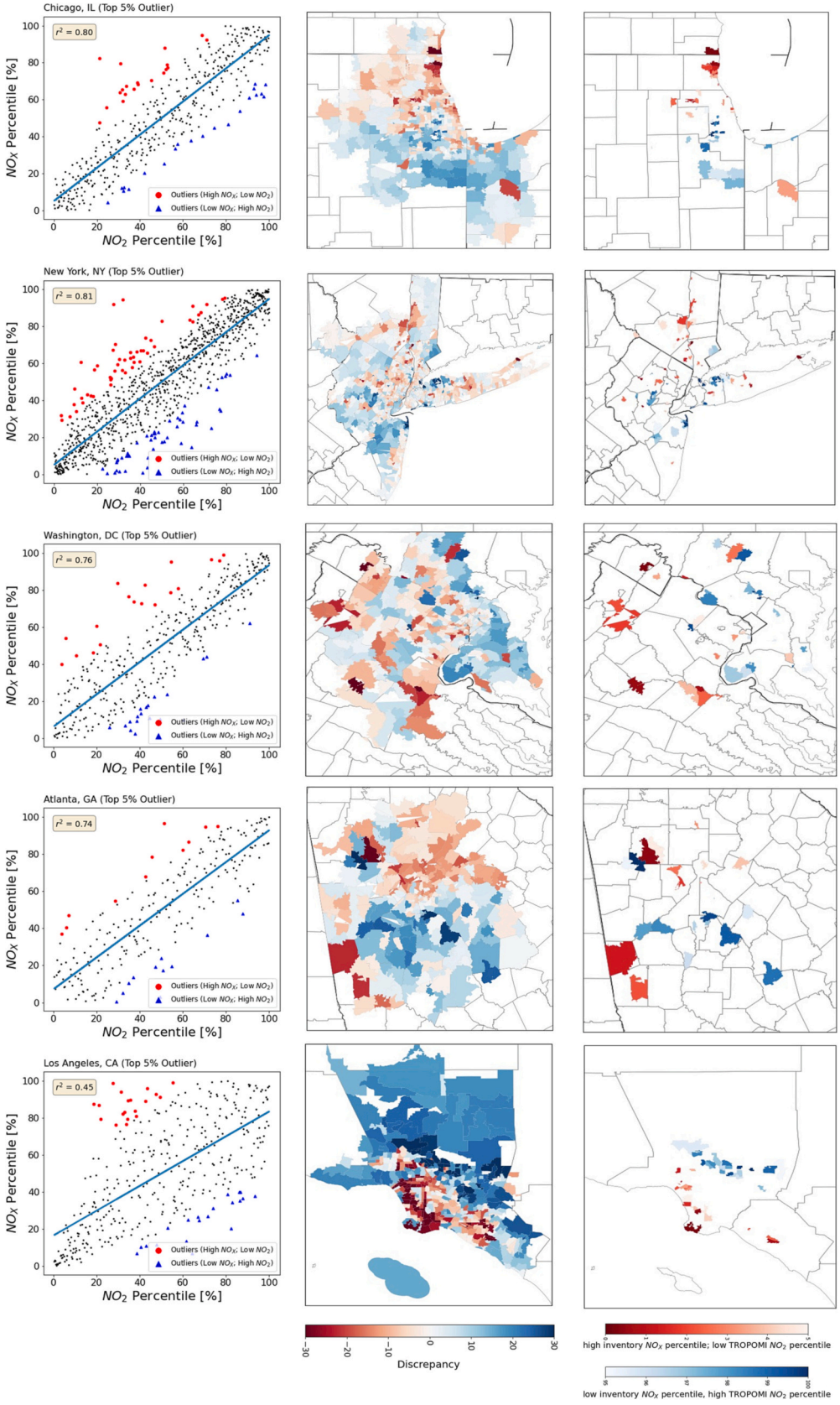

(caption on next page)

Fig. 7. Scatterplots in the left hand column compare the relative zip code percentiles within the MSA between the satellite NO_2 (x-axis) and inventory-based NOx emissions (y-axis) for (Row 1) Chicago, (Row 2) New York City, (Row 3) Washington, DC, (Row 4) Atlanta, and (Row 5) Los Angeles. Linear fit is an ordinary least squares regression. The red dots in the scatterplots represent zip codes within the MSA in which the NOx inventory percentile is a top 5% outlier, i.e., the NOx inventory percentile is substantially larger than the satellite NO_2 percentile suggesting either a NOx inventory overestimate at the zip code or that TROPOMI is unable to fully quantify the NO_2 at that location. Conversely, the blue dots in the scatterplots represent zip codes within the MSA in which the NOx inventory percentile is a bottom 5% outlier, i.e., the NOx inventory percentile is substantially smaller than the satellite NO_2 percentile suggesting either a missing source in the NOx inventory or an influence of an upwind NO_2 plume at that location. Note the different color scales between the middle and right column maps. (For interpretation of the references to color in this figure legend, the reader is referred to the web version of this article.)

Therefore, the NOx emissions in these neighborhoods may be lower in actuality than estimated in the gridded inventory-based NOx emissions. The spatial surrogates used to downscale emissions from the county-level to the zip code level may not be fully accurate with respect to the spatial distribution of vehicle type and age within the county, nor do they account for the spatial distribution of residential home heating efficiency measures. We suggest that these could be two factors to include when downscaling NOx emissions from the county-level in urban areas. Conversely, the zip codes shaded the most-blue within the MSA (60480, 60458, and 60459), suggest a NOx inventory-based underestimate west and southwest of the city. This area of the MSA is home to the largest ground package sorting facility in the world (Stagl, 2023), large intermodal railyards, a quarry, and other large industrial activities. The spatial surrogates used to downscale emissions from the county-level to a finer spatial scale may not fully account for idling vehicles and off-road equipment, such as forklifts and other heavy machinery operating at these facilities.

For all other cities – except for Los Angeles – we see similar themes emerge, albeit less pronounced, perhaps because these cities are less segregated by income. In the New York City MSA, there are red shades in Manhattan which suggests a NOx inventory overestimate, while blue shades in Staten Island suggest a NOx inventory underestimate implying a small spatial misallocation of NOx emissions within the city. We theorize that the spatial downscaling might not fully account for a heavier reliance on public transportation by those living in Manhattan relative to Staten Island residents. There is also a potential NOx emissions overestimate in the wealthier suburbs of all cities investigated: New York City (NW of the city), Washington DC (W of the city), Atlanta (N of the city), Phoenix (NE of the city), Houston (SW of the city), Dallas (NE of the city), Denver (SE of the city), and San Francisco Bay area (near Silicon Valley). Fig. 9 shows the median household income in these ten cities. Zip codes with dense warehouses, such as in central New Jersey and south of the Atlanta-Hartsfield airport, appear to have a NOx inventory underestimate. In some instances, especially in New York City, we see some disagreements along uninhabited coastline which is most likely related to NO_2 plume outflow, but could also be related to a spatial misallocation of boat/ship emissions or difficulties of the NO_2 retrieval adjacent to coastlines due to complex surface reflectivities and boundary layer dynamics (Riess et al., 2023; Sullivan et al., 2023).

Los Angeles is an outlier. We find that the NOx versus NO_2 intercomparison yields an $r^2 = 0.45$, which is substantially lower than any other US city, including the San Francisco Bay Area ($r^2 = 0.73$), which has somewhat similar climatology, or Denver ($r^2 = 0.79$), which has similar topography. We attribute the poor correlation to the complex terrain that traps the pollution locally for days/weeks. It is possible that the Los Angeles intercomparison would benefit from a high-resolution meteorological model, instead of the ERA5 $0.25^\circ \times 0.25^\circ$ re-analysis. However, we hypothesize that the persistent stagnation and accumulation of NO_2 over time within the South Coast basin may make the methodology outlined herein unfeasible. We suggest that this method should not be applied to any city that is in a "bowl-shaped" valley, such as Los Angeles, where there are complex interacting mountain and sea breezes and where pollution consistently accumulates for multiple days. Therefore, we do not attempt to make any conclusion from the inventory-based NOx versus satellite NO_2 intercomparison for Los Angeles.

We then conduct three sensitivity analyses using different filters of the TROPOMI NO_2 data: 1) restricting to summer-only and stagnant wind which effectively reduces the dataset size by a factor of four, 2) restricting to windy days (>3.2 m/s), and 3) restricting to days with unidirectionally SW wind. Correlation in the baseline scenario and the three sensitivity analyses can be seen in Table 1. The correlation between NEMO and TROPOMI generally decreases with each subsequent sensitivity analysis: r^2 decrease of 0.02 for summer-only, r^2 decrease of 0.06 for windy-only days, and r^2 decrease of 0.13 for unidirectional wind days. This suggests that a full year average using stagnant wind conditions is the most appropriate way to compare the datasets. In some cities (Chicago, New York City, Phoenix, and Denver), the correlation is above 0.70 regardless of which TROPOMI average is being used, while in other cities (DC, Atlanta, Houston, and Dallas), the correlation drops significantly when including windy days. The strong correlation in some cities during windy and unidirectional wind speed days was unexpected and is counterintuitive because days with stronger winds should disperse the NO_2 away from sources quickly. Delving into this deeper, we discover that there are large sources of NO_2 10–50 km WSW of both Chicago (near intermodal facilities, warehouses, and industrial operations) and New York City (Newark port / warehouses) effectively moving the NO_2 from the NOx emissions on the SW side to directly over the city, giving the appearance that the largest NOx is originating over the city center when in fact it is an accumulation of upwind and local NO_X emissions. This can be best seen in the spatial plots showing SW winds – the climatologically dominant wind direction in these two cities. On days with SW winds, there are meaningful NO_2 enhancements upwind of the urban cores of Chicago and New York City (Fig. 10). Since population density is a large driver of the inventory downscaling – from the county-level to 1-km – it is possible that the prevailing wind direction is falsely giving an appearance of better agreement between the inventory and satellite data.

4. Discussion

This analysis demonstrates that TROPOMI NO_2 when oversampled during stagnant wind days over multiple years can be an effective surrogate to estimate the spatial heterogeneities of NOx emissions within an urban area. In nine of the ten US cities analyzed here, r^2-values between the NEMO NOx inventory and TROPOMI NO_2 apportioned by percentile exceeded 0.73. This finding suggests that the 108 spatial surrogates used to spatially disaggregate NOx emissions from the U.S. county-level (~25 km length scale) to the neighborhood level (~1 km length scale) are generally appropriate, especially for modeling applications with a 12 km spatial resolution or coarser. However, this analysis also suggests some areas for improvement in the inventories. We find that areas that have a large density of warehouse operations appear to underestimate NOx emissions. This may be partially due to the proliferation of large warehouse construction since 2017, the year for which the NEI was developed. Nonetheless, this analysis suggests that characterizing the sources and magnitudes of NOx emissions near warehouses should be a priority for future research, as consumers and retailers continue to push for same-day home delivery of goods. Conversely, we find some evidence that NOx emissions in wealthy communities may be overestimated using standard surrogates to disaggregate the inventory. Wealthier residents are more likely to own newer vehicles with better catalytic converters, own newer homes or have the ability to install home heating energy efficiency measures, own electrified tools/vehicles, and have the

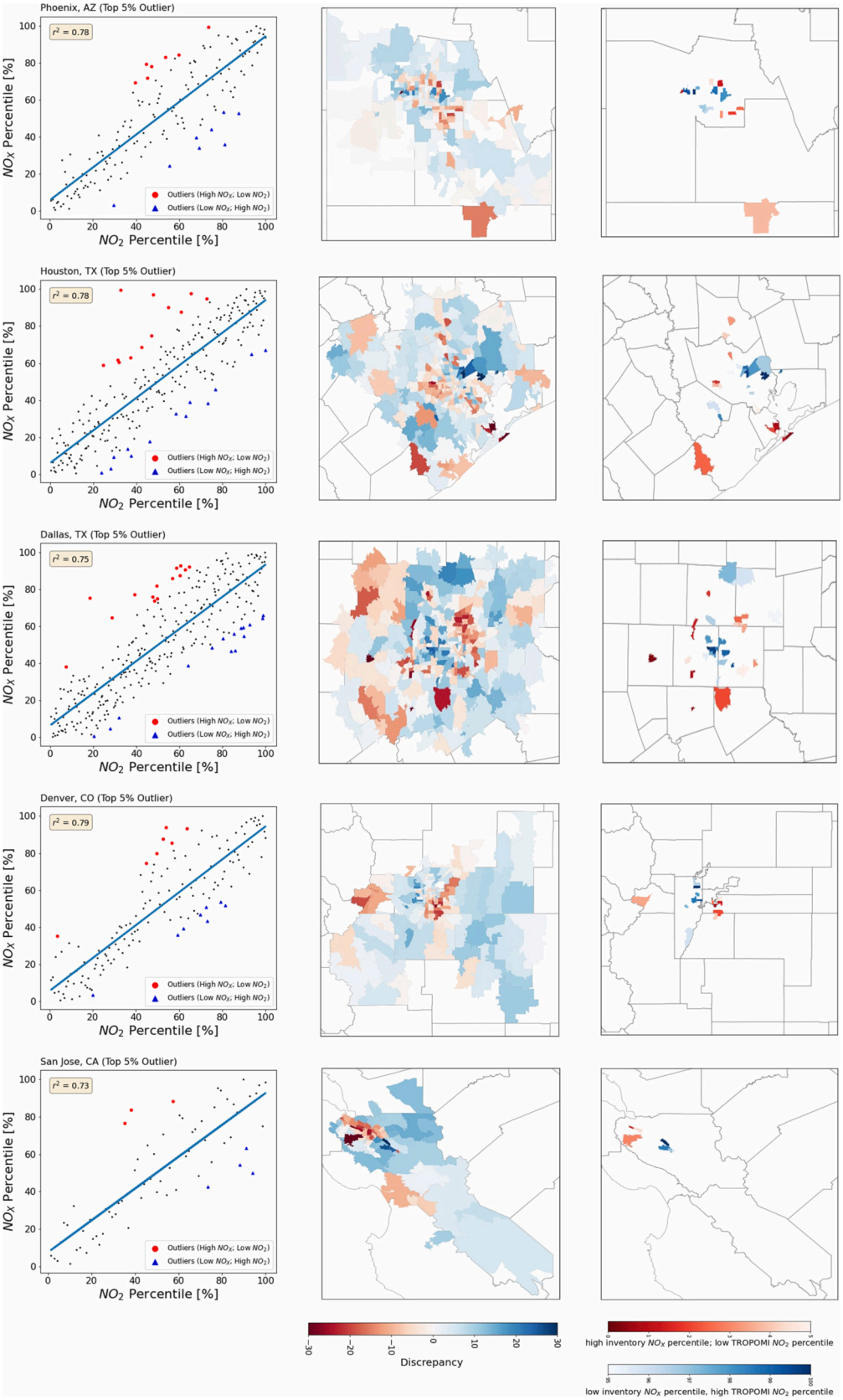

Fig. 8. Same as Fig. 7 but now showing: (Row 1) Phoenix, (Row 2) Houston, (Row 3) Dallas, (Row 4) Denver, and (Row 5) San Francisco Bay Area.

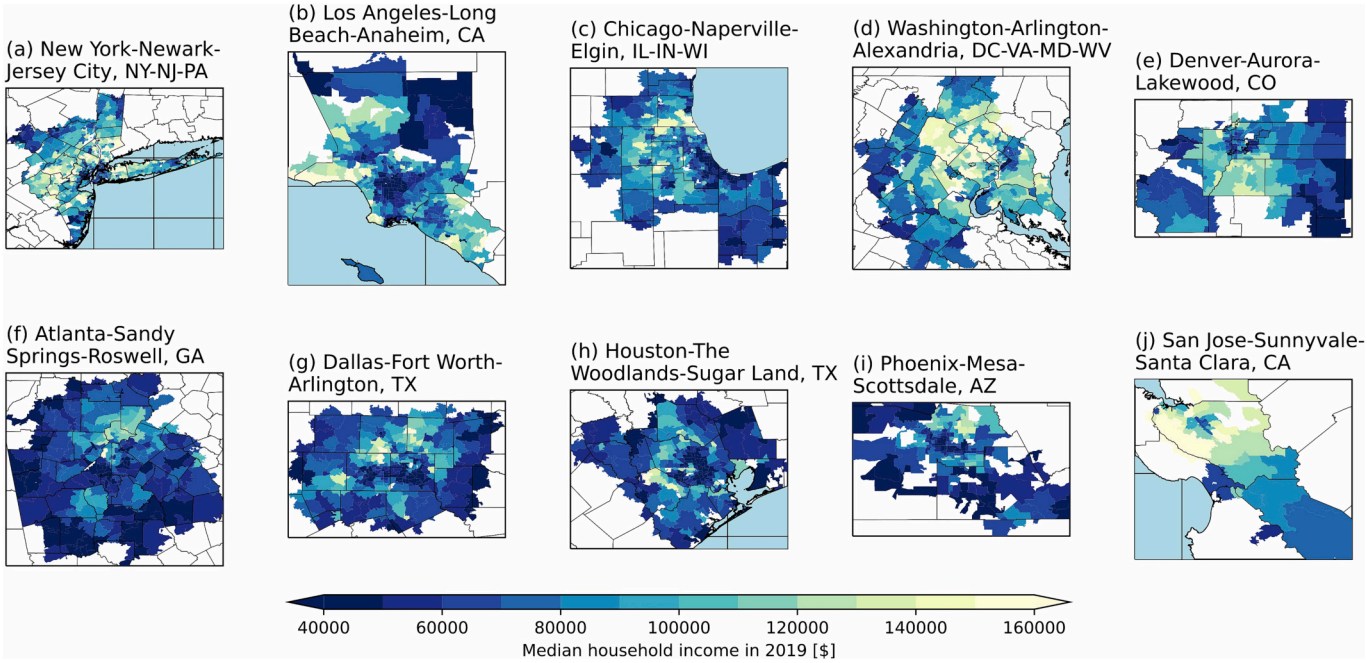

Fig. 9. Median household income by zip code in 2019 for the ten focus cities from the American Community Survey as processed by Manson et al. (2022).

Table 1
Correlation of NEMO vs. TROPOMI using the "baseline" TROPOMI NO_2 filter and three different "sensitivity" filtering criteria. Correlation in the "All Days & Stagnant" column are the same correlations shown in Figs. 7 & 8.

	Correlation: NEMO vs. TROPOMI			
	All Days & Stagnant Wind	Summer & Stagnant Wind	All Days & Windy	All Days & Unidirectional
Chicago	0.80	0.78	0.79	0.79
NYC	0.81	0.81	0.77	0.72
DC	0.76	0.76	0.65	0.65
Atlanta	0.74	0.71	0.62	0.57
LA	0.45	0.30	0.32	0.28
Phoenix	0.78	0.85	0.77	0.77
Houston	0.78	0.76	0.73	0.41
Dallas	0.75	0.75	0.71	0.52
Denver	0.79	0.82	0.83	0.74
San Jose	0.73	0.62	0.58	0.63
Average difference		−0.02	−0.06	−0.13

political capital to minimize emitters, such as diesel trucks, within their neighborhood.

In many gridded emissions inventories, population-related data are used as surrogates to downscale emissions. While this approach is appropriate in some cases when other information, such as ownership of fossil-fuel-based machinery is not known, our results suggest that including a median household income spatial surrogate for the on-road, non-road, and residential heating sectors may further improve the spatial allocation of these emissions. This is an important finding for two reasons. First, this suggests that the standard assumptions to downscale NOx emissions may not be fully appropriate for some applications, such as evaluating pollution disparities between advantaged and disadvantaged communities. Second, this finding suggests that more work needs to be done to develop emission reduction strategies that target lower socioeconomic neighborhoods rather than applying citywide standards that may disproportionately benefit neighborhoods that already have relatively low emissions. Pinpointing NOx emissions may be less useful for ozone simulations since ozone is a more homogenous pollutant, but it is possible that modifying the spatial distribution of urban NOx emissions could affect ozone formation sensitivity within different sections of the metropolitan area.

From a remote sensing perspective, this work demonstrates that satellite data can be useful in evaluating a NOx emissions inventory without the use of a chemical transport model or complex statistical manipulation under certain conditions. Such comparisons should use a long-term average of satellite data because there would be too much missing data, random noise, and unaccounted meteorological effects if only one day or one month were used. If possible, we find that it's more appropriate to isolate days with slow wind speeds and average them together, rather than averaging all days without accounting for winds. This is because winds disperse NOx, leading to spatial offsets between where the NOx was emitted and where the satellite will observe it. We find that restricting the satellite dataset to a summer-only is unnecessary, since there are similar NO_2 spatial distributions with and without this restriction, even though the NO_2 magnitude is smaller during summer. In addition, the climatological/prevailing wind direction, such as climatological southwesterly winds in New York City and Chicago, can give the appearance of a false agreement.

While we use the operational TROPOMI NO_2 version 2.4 algorithm, we note that using NO_2 vertical shape profiles from a high-resolution chemical transport model to re-process the satellite air mass factor for the urban measurements would have been ideal and may yield slightly different correlation in the urban areas. Re-processing the air mass factor using a high spatial resolution simulation generally increases NO_2 for urban/polluted measurements while rural/unpolluted measurements remain similar (Douros et al., 2023; Goldberg et al., 2017; Goldberg et al., 2019c; Judd et al., 2020), and therefore has the net effect of increasing the range of the NO_2 magnitudes in an metropolitan area but has little effect on the percentiles within a metropolitan area.

This work demonstrates how satellite data can be helpful for policymakers in characterizing the spatial distribution of NOx emissions without a chemical transport model. The improved spatial resolution and reduced noise of TROPOMI enables a new way to evaluate NOx emission inventories in urban areas at scales previously not possible. Future instruments, such as TEMPO and Sentinel 4, with similar pixel sizes, but more numerous observations (hourly measurements instead of a single daily measurement), may allow this comparison to be done on shorter timeframes.

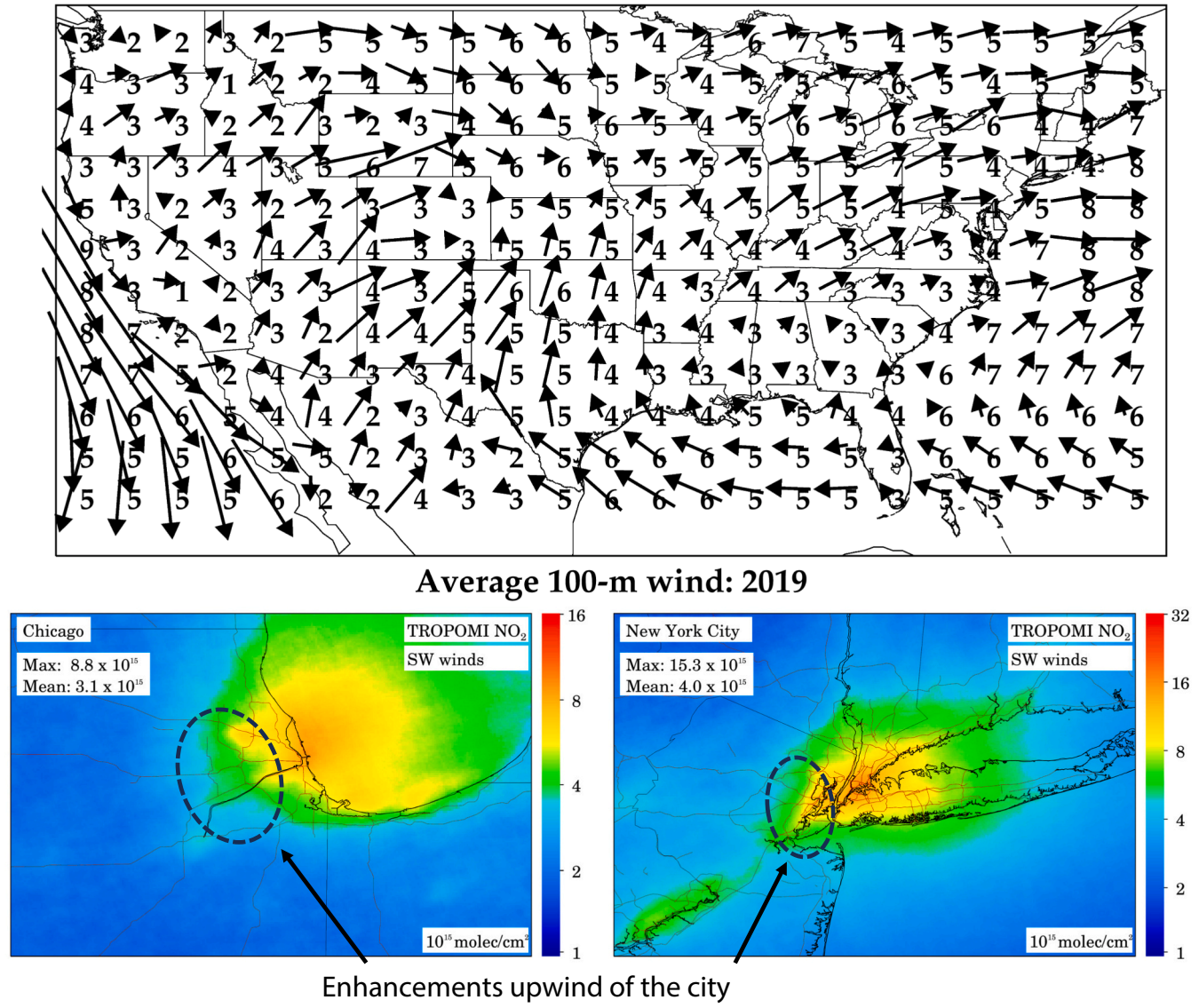

Fig. 10. Top panel shows the 2019 climatological wind direction and speed in m-s^{-1}. Bottom panels show TROPOMI NO_2 when filtering to show southwest (SW) winds only in the Chicago and New York City metropolitan areas.

CRediT authorship contribution statement

Daniel L. Goldberg: Conceptualization, Methodology, Software, Formal analysis, Data curation, Writing – original draft, Writing – review & editing, Visualization, Project administration, Funding acquisition. **Madankui Tao:** Software, Formal analysis, Data curation, Writing – review & editing, Visualization. **Gaige Kerr:** Software, Formal analysis, Data curation, Writing – review & editing, Visualization. **Siqi Ma:** Data curation, Writing – review & editing. **Daniel Tong:** Data curation, Writing – review & editing. **Arlene M. Fiore:** Writing – review & editing, Project administration, Funding acquisition. **Angela F. Dickens:** Writing – review & editing. **Zachariah Adelman:** Writing – review & editing. **Susan Anenberg:** Writing – review & editing, Project administration, Funding acquisition.

Declaration of Competing Interest

The authors declare the following financial interests/personal relationships which may be considered as potential competing interests:

Daniel Goldberg reports financial support was provided by NASA.

Data availability

Data will be made available on request.

Acknowledgments

Preparation of this manuscript was funded by grants from the NASA Health and Air Quality Applied Sciences Team (HAQAST) (80NSSC21K0511 & 80NSSC21K0509), NASA Health and Air Quality (HAQ) (80NSSC19K0193), and the NASA Atmospheric Composition Modeling and Analysis Program (ACMAP) (80NSSC19K0946). We appreciate feedback from Mark Janssen on the intercomparison in the Chicago area. TROPOMI NO_2 v2.4 (https://doi.org/10.5270/S5P-9bnp8q8) data can be freely downloaded via APIs in the Copernicus Data Space Ecosystem (https://dataspace.copernicus.eu/).. ERA5 reanalysis hourly data on single levels (doi: 10.24381/cds.adbb2d47) can be downloaded from Copernicus Climate Data Store (https://cds.climate.copernicus.eu/#!/home). IDL code to re-grid and process the data is available upon request.

References

Anenberg, S.C., Mohegh, A., Goldberg, D.L., Kerr, G.H., Brauer, M., Burkart, K., et al., 2022. Long-term trends in urban NO2 concentrations and associated paediatric asthma incidence: estimates from global datasets. Lancet Planet. Health 6 (1), e49–e58. https://doi.org/10.1016/S2542-5196(21)00255-2.

Beirle, S., Boersma, K.F., Platt, U., Lawrence, M.G., Wagner, T., 2011. Megacity emissions and lifetimes of nitrogen oxides probed from space. Science 333 (6050), 1737–1739. https://doi.org/10.1126/science.1207824.

Beirle, S., Borger, C., Dörner, S., Li, A., Hu, Z., Liu, F., et al., 2019. Pinpointing nitrogen oxide emissions from space. Sci. Adv. 5 (11), eaax9800 https://doi.org/10.1126/sciadv.aax9800.

Beirle, S., Borger, C., Jost, A., Wagner, T., 2023. Improved catalog of NOx point source emissions (version 2). Earth Syst. Sci. Data 15 (7), 3051–3073. https://doi.org/10.5194/essd-15-3051-2023.

Boersma, K.F., Eskes, H.J., Dirksen, R.J., Van Der, A.R.J., Veefkind, J.P., Stammes, P., et al., 2011. An improved tropospheric NO2 column retrieval algorithm for the ozone monitoring instrument. Atmos. Meas. Tech. 4 (9), 1905–1928. https://doi.org/10.5194/amt-4-1905-2011.

Boersma, K.F., Eskes, H.J., Richter, A., De Smedt, I., Lorente, A., Beirle, S., et al., 2018. Improving algorithms and uncertainty estimates for satellite NO2 retrievals: results from the quality assurance for the essential climate variables (QA4ECV) project. Atmos. Meas. Tech. 11 (12), 6651–6678. https://doi.org/10.5194/amt-11-6651-2018.

Burnett, R.T., Stieb, D., Brook, J.R., Cakmak, S., Dales, R., Raizenne, M., et al., 2004. Associations between short-term changes in nitrogen dioxide and mortality in Canadian cities. Arch. Environ. Health 59 (5), 228–236. https://doi.org/10.3200/AEOH.59.5.228-236.

Busca, G., Lietti, L., Ramis, G., Berti, F., 1998. Chemical and mechanistic aspects of the selective catalytic reduction of NO(x) by ammonia over oxide catalysts: a review. Appl. Catal. B Environ. 18 (1–2), 1–36. https://doi.org/10.1016/S0926-3373(98)00040-X.

Canty, T.P., Hembeck, L., Vinciguerra, T.P., Anderson, D.C., Goldberg, D.L., Carpenter, S. F., et al., 2015. Ozone and NOx chemistry in the eastern US: evaluation of CMAQ/CB05 with satellite (OMI) data. Atmos. Chem. Phys. 15 (19), 10965–10982. https://doi.org/10.5194/acp-15-10965-2015.

Chen, Y.-C., Chou, C.C.K., Liu, C.-Y., Chi, S.-Y., Chuang, M.-T., 2023. Evaluation of the nitrogen oxide emission inventory with TROPOMI observations. Atmos. Environ. 119639 https://doi.org/10.1016/J.ATMOSENV.2023.119639.

Crippa, M., Guizzardi, D., Muntean, M., Schaaf, E., Dentener, F., van Aardenne, J.A., et al., 2018. Gridded emissions of air pollutants for the period 1970–2012 within EDGAR v4.3.2. Earth Syst. Sci. Data 10 (4), 1987–2013. https://doi.org/10.5194/essd-10-1987-2018.

Crippa, M., Guizzardi, D., Pisoni, E., Solazzo, E., Guion, A., Muntean, M., et al., 2021. Global anthropogenic emissions in urban areas: patterns, trends, and challenges. Environ. Res. Lett. 16 (7), 074033 https://doi.org/10.1088/1748-9326/AC00E2.

de Foy, B., Krotkov, N.A., Bei, N., Herndon, S.C., Huey, L.G., Martínez, A.-P., et al., 2009. Hit from both sides: tracking industrial and volcanic plumes in Mexico City with surface measurements and OMI SO2 retrievals during the MILAGRO field campaign. Atmos. Chem. Phys. 9 (24), 9599–9617. https://doi.org/10.5194/acp-9-9599-2009.

Demetillo, M.A.G., Navarro, A., Knowles, K.K., Fields, K.P., Geddes, J.A., Nowlan, C.R., et al., 2020. Observing nitrogen dioxide air pollution inequality using high-spatial-resolution remote sensing measurements in Houston, Texas. Environ. Sci. Technol. 54 (16), 9882–9895. https://doi.org/10.1021/acs.est.0c01864.

Douros, J., Eskes, H., Van Geffen, J., Folkert Boersma, K., Compernolle, S., Pinardi, G., et al., 2023. Comparing Sentinel-5P TROPOMI NO2 column observations with the CAMS regional air quality ensemble. Geosci. Model Dev. 16, 509–534. https://doi.org/10.5194/gmd-16-509-2023.

Dressel, I.M., Demetillo, M.A.G., Judd, L.M., Janz, S.J., Fields, K.P., Sun, K., et al., 2022. Daily satellite observations of nitrogen dioxide air pollution inequality in New York City, New York and Newark, New Jersey: evaluation and application. Environ. Sci. Technol. 2022 https://doi.org/10.1021/ACS.EST.2C02828/ASSET/IMAGES/LARGE/ES2C02828_0006.JPEG.

East, J.D., Henderson, B.H., Napelenok, S.L., Koplitz, S.N., Sarwar, G., Gilliam, R., et al., 2022. Inferring and evaluating satellite-based constraints on NOx emissions estimates in air quality simulations. Atmos. Chem. Phys. 22, 15981–16001. https://doi.org/10.5194/acp-22-15981-2022.

Eskes, H.J., Eichmann, K.-U., Lambert, J.-C., Loyola, D., Stein-Zweers, D., Dehn, A., Zehner, C., 2023. S5P MPC Product Readme Nitrogen Dioxide. https://doi.org/10.5270/S5P-9bnp8q8.

Eyth, A., Ran, L., Partheepan, R., Yarwood, G., 2006. New Tools to Generate Spatial Surrogate and Speciation Profile Inputs to SMOKE.

Federal Highway Administration, 2018. 2017 National Household Travel Survey. Retrieved October 2, 2023, from https://nhts.ornl.gov/.

Finch, D.P., Palmer, P.I., Zhang, T., 2022. Automated detection of atmospheric NO2 plumes from satellite data: a tool to help infer anthropogenic combustion emissions. Atmos. Meas. Tech. 15 (3), 721–733. https://doi.org/10.5194/AMT-15-721-2022.

Geddes, J.A., Wang, B., Li, D., 2021. Ozone and nitrogen dioxide pollution in a coastal urban environment: the role of sea breezes, and implications of their representation for remote sensing of local air quality. J. Geophys. Res. Atmos. 126 (18), e2021JD035314 https://doi.org/10.1029/2021JD035314.

Goldberg, D.L., Lamsal, L.N., Loughner, C.P., Swartz, W.H., Lu, Z., Streets, D.G., 2017. A high-resolution and observationally constrained OMI NO2 satellite retrieval. Atmos. Chem. Phys. 17 (18), 11403–11421. https://doi.org/10.5194/acp-17-11403-2017.

Goldberg, D.L., Lu, Z., Oda, T., Lamsal, L.N., Liu, F., Griffin, D., et al., 2019a. Exploiting OMI NO2 satellite observations to infer fossil-fuel CO2 emissions from U.S. megacities. Sci. Total Environ. 695, 133805 https://doi.org/10.1016/j.scitotenv.2019.133805.

Goldberg, D.L., Lu, Z., Streets, D.G., de Foy, B., Griffin, D., McLinden, C.A., et al., 2019b. Enhanced capabilities of TROPOMI NO2: estimating NOx from North American cities and power plants. Environ. Sci. Technol. 53 (21), 12594–12601. https://doi.org/10.1021/acs.est.9b04488.

Goldberg, D.L., Saide, P.E., Lamsal, L.N., de Foy, B., Lu, Z., Woo, J.-H., et al., 2019c. A top-down assessment using OMI NO2 suggests an underestimate in the NOx emissions inventory in Seoul, South Korea, during KORUS-AQ. Atmos. Chem. Phys. 19 (3), 1801–1818. https://doi.org/10.5194/acp-19-1801-2019.

Goldberg, D.L., Anenberg, S.C., Kerr, G.H., Mohegh, A., Lu, Z., Streets, D.G., 2021a. TROPOMI NO2 in the United States: a detailed look at the annual averages, weekly cycles, effects of temperature, and correlation with surface NO 2 concentrations. Earth's Future 9 (4), e2020EF001665. https://doi.org/10.1029/2020EF001665.

Goldberg, D.L., Anenberg, S.C., Lu, Z., Streets, D.G., Lamsal, L.N.E., McDuffie, E., Smith, S.J., 2021b. Urban NOx emissions around the world declined faster than anticipated between 2005 and 2019. Environ. Res. Lett. 16 (11), 115004 https://doi.org/10.1088/1748-9326/ac2c34.

Goldberg, D.L., Harkey, M., de Foy, B., Judd, L., Johnson, J., Yarwood, G., Holloway, T., 2022. Evaluating NOx emissions and their effect on O3 production in Texas using TROPOMI NO2 and HCHO. Atmos. Chem. Phys. 22 (16), 10875–10900. https://doi.org/10.5194/acp-22-10875-2022.

Guttikunda, S.K., Nishadh, K.A., Jawahar, P., 2019. Air pollution knowledge assessments (APnA) for 20 Indian cities. Urban Clim. 27, 124–141. https://doi.org/10.1016/j.uclim.2018.11.005.

He, M.Z., Kinney, P.L., Li, T., Chen, C., Sun, Q., Ban, J., et al., 2020. Short- and intermediate-term exposure to NO2 and mortality: a multi-county analysis in China. Environ. Pollut. 261, 114165 https://doi.org/10.1016/j.envpol.2020.114165.

Health Effects Institute, 2022. Systematic Review and Meta-analysis of Selected Health Effects of Long-Term Exposure to Traffic-Related Air Poll. Retrieved from https://www.healtheffects.org/system/files/hei-special-report-23-executive-summary_0.pdf.

Hersbach, H., Bell, B., Berrisford, P., Hirahara, S., Horányi, A., Muñoz-Sabater, J., et al., 2020. The ERA5 global reanalysis. Q. J. R. Meteorol. Soc. 146 (730), 1999–2049. https://doi.org/10.1002/qj.3803.

Janssens-Maenhout, G., Crippa, M., Guizzardi, D., Dentener, F., Muntean, M., Pouliot, G., et al., 2015. HTAP_v2.2: a mosaic of regional and global emission grid maps for 2008 and 2010 to study hemispheric transport of air pollution. Atmos. Chem. Phys. 15 (19), 11411–11432. https://doi.org/10.5194/acp-15-11411-2015.

Joint Research Centre, 2022. Emissions Database for Global Atmospheric Research Version 6.1. Retrieved from https://edgar.jrc.ec.europa.eu/index.php/dataset_ap61.

Judd, L.M., Al-Saadi, J.A., Szykman, J.J., Valin, L.C., Janz, S.J., Kowalewski, M.G., et al., 2020. Evaluating sentinel-5P TROPOMI tropospheric NO2 column densities with airborne and Pandora spectrometers near New York City and Long Island sound. Atmos. Meas. Tech. 13 (11), 6113–6140. https://doi.org/10.5194/amt-13-6113-2020.

Kerr, G.H., Goldberg, D.L., Anenberg, S.C., 2021. COVID-19 pandemic reveals persistent disparities in nitrogen dioxide pollution. Proc. Natl. Acad. Sci. 118 (30), e2022409118 https://doi.org/10.1073/pnas.2022409118.

Khreis, H., Kelly, C., Tate, J., Parslow, R., Lucas, K., Nieuwenhuijsen, M., 2017. Exposure to traffic-related air pollution and risk of development of childhood asthma: a systematic review and meta-analysis. Environ. Int. 100, 1–31. https://doi.org/10.1016/j.envint.2016.11.012.

Koltsakis, G., Stamatelos, A., 1997. Catalytic automotive exhaust aftertreatment. Prog. Energy Combust. Sci. 23 (1), 1–39. https://doi.org/10.1016/s0360-1285(97)00003-8.

Lambert, J.-C., Claas, J., Stein-Zweers, D., Ludewig, A., Loyola, D., Sneep, M., Dehn, A., 2023. Quarterly Validation Report of the Copernicus Sentinel-5 Precursor Operational Data Products #19.

Laughner, J.L., Cohen, R.C., 2019. Direct observation of changing NOx lifetime in North American cities. Science 366 (6466), 723–727. https://doi.org/10.1126/science.aax6832.

Lee, J.H., Hardman, S.J., Tal, G., 2019. Who is buying electric vehicles in California? Characterising early adopter heterogeneity and forecasting market diffusion. Energy Res. Soc. Sci. 55, 218–226. https://doi.org/10.1016/j.erss.2019.05.011.

Levelt, P.F., Joiner, J., Tamminen, J., Veefkind, J.P., Bhartia, P.K., Zweers, D.C.S., et al., 2018. The ozone monitoring instrument: overview of 14 years in space. Atmos. Chem. Phys. 18 (8), 5699–5745. https://doi.org/10.5194/acp-18-5699-2018.

Li, M., McDonald, B.C., McKeen, S.A., Eskes, H.J., Levelt, P., Francoeur, C., et al., 2021. Assessment of updated fuel-based emissions inventories over the contiguous United States using TROPOMI NO 2 retrievals. J. Geophys. Res. Atmos. 126 (24) https://doi.org/10.1029/2021JD035484 e2021JD035484.

Liu, F., Beirle, S., Zhang, Q., Van Der, A.R.J., Zheng, B., Tong, D., He, K., 2017. NOx emission trends over Chinese cities estimated from OMI observations during 2005 to 2015. Atmos. Chem. Phys. 17 (15), 9261–9275. https://doi.org/10.5194/acp-17-9261-2017.

Liu, S., Valks, P., Pinardi, G., Xu, J., Chan, K.L., Argyrouli, A., et al., 2021. An improved TROPOMI tropospheric NO2 research product over Europe. Atmos. Meas. Tech. 14 (11), 7297–7327. https://doi.org/10.5194/amt-14-7297-2021.

Liu, F., Tao, Z., Beirle, S., Joiner, J., Yoshida, Y., Smith, S.J., et al., 2022. A new method for inferring city emissions and lifetimes of nitrogen oxides from high-resolution nitrogen dioxide observations: a model study. Atmos. Chem. Phys. 22, 1333–1349. https://doi.org/10.5194/acp-22-1333-2022.

Lorente, A., Folkert Boersma, K., Yu, H., Dörner, S., Hilboll, A., Richter, A., et al., 2017. Structural uncertainty in air mass factor calculation for NO2 and HCHO satellite retrievals. Atmos. Meas. Tech. 10 (3), 759–782. https://doi.org/10.5194/amt-10-759-2017.

Lorente, A., Boersma, K.F., Eskes, H.J., Veefkind, J.P., van Geffen, J.H.G.M., de Zeeuw, M.B., et al., 2019. Quantification of nitrogen oxides emissions from build-up of pollution over Paris with TROPOMI. Sci. Rep. 9 (1), 20033. https://doi.org/10.1038/s41598-019-56428-5.

Ma, S., Tong, D.Q., 2022. Neighborhood Emission Mapping Operation (NEMO): a 1-km anthropogenic emission dataset in the United States. Sci. Data 9 (1), 1–10. https://doi.org/10.1038/s41597-022-01790-9.

Manson, S., Schroeder, J., Van Riper, D., Ruggles, S., 2022. IPUMS National Historical Geographic Information System: Version 17.0. Minneapolis, MN. https://doi.org/10.18128/D050.V17.0.

McDuffie, E.E., Smith, S.J., O'Rourke, P., Tibrewal, K., Venkataraman, C., Marais, E.A., et al., 2020. A global anthropogenic emission inventory of atmospheric pollutants from sector- and fuel-specific sources (1970–2017): an application of the Community Emissions Data System (CEDS). Earth Syst. Sci. Data 12 (4), 3413–3442. https://doi.org/10.5194/essd-12-3413-2020.

Miller, T.L., Davis, W.T., Reed, G.D., Doraiswamy, P., Tang, A., 2002. Effect of county-level income on vehicle age distribution and emissions. Trans. Res. Rec. J. Transp. Res. Board 1815 (1), 47–53. https://doi.org/10.3141/1815-06.

Montgomery, A., Daepp, M.I.G., Abdin, M.I., Choudhury, P., Malvar, S., Counts, S., Horton, D.E., 2023. Intraurban NO2 hotspot detection across multiple air quality products. Environ. Res. Lett. https://doi.org/10.1088/1748-9326/acf7d5.

Palmer, P.I., Jacob, D.J., Chance, K.V., Martin, R.V., Spurr, R.J.D., Kurosu, T.P., et al., 2001. Air mass factor formulation for spectroscopic measurements from satellites: application to formaldehyde retrievals from the Global Ozone Monitoring Experiment. J. Geophys. Res. Atmos. 106 (D13), 14539–14550. https://doi.org/10.1029/2000JD900772.

Platt, U., 1994. Differential optical absorption spectroscopy (DOAS). In: Air Monitoring by Spectroscopic Techniques. Wiley-IEEE, p. 531.

Pope, R.J., Kelly, R., Marais, E.A., Graham, A.M., Wilson, C., Harrison, J.J., et al., 2022. Exploiting satellite measurements to explore uncertainties in UK bottom-up NOx emission estimates. Atmos. Chem. Phys. 22 (7), 4323–4338. https://doi.org/10.5194/ACP-22-4323-2022.

Richter, A., Begoin, M., Hilboll, A., Burrows, J.P., 2011. An improved NO2 retrieval for the GOME-2 satellite instrument. Atmos. Meas. Tech. 4 (6), 1147–1159. https://doi.org/10.5194/amt-4-1147-2011.

Riess, T.C.V.W., Folkert Boersma, K., Van Roy, W., De Laat, J., Dammers, E., Van Vliet, J., 2023. To new heights by flying low: comparison of aircraft vertical NO2 profiles to model simulations and implications for TROPOMI NO2 retrievals. EGUsphere. https://doi.org/10.5194/egusphere-2023-1059.

Saw, G.K., Dey, S., Kaushal, H., Lal, K., 2021. Tracking NO2 emission from thermal power plants in North India using TROPOMI data. Atmos. Environ. 259, 118514 https://doi.org/10.1016/j.atmosenv.2021.118514.

Solari, C.D., 2012. Affluent neighborhood persistence and change in U.S. Cities. City Community 11 (4), 370–388. https://doi.org/10.1111/j.1540-6040.2012.01422.x.

Stagl, J., 2023. UPS Relies Heavily on Railroads to Keep the Giant Chicago Area Consolidation Hub on Schedule. Retrieved September 21, 2023, from https://www.progressiverailroading.com/intermodal/article/UPS-relies-heavily-on-railroads-to-keep-the-giant-Chicago-Area-Consolidation-Hub-on-schedule–37645.

Sullivan, J.T., Stauffer, R.M., Thompson, A.M., Tzortziou, M.A., Loughner, C.P., Jordan, C.E., Santanello, J.A., 2023. Surf, turf, and above the earth: unmet needs for coastal air quality science in the planetary boundary layer (PBL). Earth's Future 11 (6). https://doi.org/10.1029/2023EF003535.

Sun, K., Zhu, L., Cady-Pereira, K.E., Chan Miller, C., Chance, K.V., Clarisse, L., et al., 2018. A physics-based approach to oversample multi-satellite, multi-species observations to a common grid. Atmos. Measure. Tech. Discuss. 11 (12), 1–30. https://doi.org/10.5194/amt-2018-253.

Sun, K., Li, L., Jagini, S., Li, D., 2021. A satellite-data-driven framework to rapidly quantify air-basin-scale NOx emissions and its application to the Po Valley during the COVID-19 pandemic. Atmos. Chem. Phys. 21 (17), 13311–13332. https://doi.org/10.5194/ACP-21-13311-2021.

U.S. Census Bureau, 2022. 2021 American Housing Survey. Retrieved October 2, 2023, from https://www.census.gov/programs-surveys/ahs.html.

van Geffen, J., 2016. TROPOMI ATBD of the Total and Tropospheric NO2 Data Products, (2). Retrieved from https://sentinel.esa.int/documents/247904/2476257/Sentinel-5P-TROPOMI-ATBD-NO2-data-products.

van Geffen, J., Boersma, K.F., Eskes, H.J., Sneep, M., ter Linden, M., Zara, M., Veefkind, J.P., 2020. S5P TROPOMI NO2 slant column retrieval: method, stability, uncertainties and comparisons with OMI. Atmos. Meas. Tech. 13 (3), 1315–1335. https://doi.org/10.5194/amt-13-1315-2020.

van Geffen, J., Eskes, H.J., Compernolle, S., Pinardi, G., Verhoelst, T., Lambert, J.-C., et al., 2021. Sentinel-5P TROPOMI NO2 retrieval: impact of version v2.2 improvements and comparisons with OMI and ground-based data. Atmos. Meas. Tech. 15 (7), 2037–2060. https://doi.org/10.5194/AMT-15-2037-2022.

Vandaele, A.C., Hermans, C., Simon, P.C., Carleer, M., Colin, R., Fally, S., et al., 1998. Measurements of the NO2 absorption cross-section from 42 000 cm−1 to 10 000 cm−1 (238–1000 nm) at 220 K and 294 K. J. Quant. Spectrosc. Radiat. Transf. 59 (3–5), 171–184. https://doi.org/10.1016/S0022-4073(97)00168-4.

Veefkind, J.P., Aben, I., McMullan, K., Förster, H., de Vries, J., Otter, G., et al., 2012. TROPOMI on the ESA Sentinel-5 Precursor: a GMES mission for global observations of the atmospheric composition for climate, air quality and ozone layer applications. Remote Sens. Environ. 120 (2012), 70–83. https://doi.org/10.1016/j.rse.2011.09.027.

Verstraeten, W.W., Boersma, K.F., Douros, J., Williams, J.E., Eskes, H., Liu, F., et al., 2018. Top-down NOX emissions of European cities based on the downwind plume of modelled and space-borne tropospheric NO2 columns. Sensors 18 (9), 2893. https://doi.org/10.3390/s18092893.

Wang, B., Geddes, J.A., Adams, T.J., Lind, E.S., McDonald, B.C., He, J., et al., 2023. Implications of sea breezes on air quality monitoring in a coastal urban environment: evidence from high resolution modeling of NO2 and O3. J. Geophys. Res. Atmos., e2022JD037860 https://doi.org/10.1029/2022JD037860.

Xu, X., Chen, C. Fei, 2019. Energy efficiency and energy justice for U.S. low-income households: an analysis of multifaceted challenges and potential. Energy Policy 128, 763–774. https://doi.org/10.1016/j.enpol.2019.01.020.

Xue, R., Wang, S., Zhang, S., He, S., Liu, J., Tanvir, A., Zhou, B., 2022. Estimating city NOx emissions from TROPOMI high spatial resolution observations – a case study on Yangtze River Delta, China. Urban Clim. 43, 101150 https://doi.org/10.1016/J.UCLIM.2022.101150.